


Deciphering the minimal quantity of mouse primary cells to undergo nephrogenesis ex vivo

Aleksandra Rak-Raszewska¹  | Ganna Reint¹ | Fabienne Geiger¹ | Florence Naillat¹ | Seppo J. Vainio^{1,2}

¹Laboratory of Developmental Biology, Disease Networks Research Unit, Faculty of Biochemistry and Molecular Medicine, University of Oulu, Oulu, Finland

²Kvantum Institute, Infotech Oulu, University of Oulu, Oulu, Finland

Correspondence

Aleksandra Rak-Raszewska, Laboratory of Developmental Biology, Disease Networks Research Unit, Faculty of Biochemistry and Molecular Medicine, University of Oulu, Aapistie 5, 90220 Oulu, Finland.
Email: aleksandra.rak-raszewska@oulu.fi; a.rakraszewska@gmail.com

Funding information

This work was supported by Finnish Cultural Foundation (#00160821 personal grant to Aleksandra Rak-Raszewska), CIMO Fellowship (personal grant to Ganna Reint), Center of Excellence grant (#2513149) and Academy of Finland Grant (315030).

Abstract

Background: Tissue organoids derived from primary cells have high potential for studying organ development and diseases in numerous organs. They recreate the morphological structure and mimic the functions of given organ while being compact in size, easy to produce, and suitable for use in various experimental setups.

Results: In this study we established the number of cells that form mouse kidney rudiments at E11.5, and generated renal organoids of various sizes from the mouse primary cells of the metanephric mesenchyme (MM). We investigated the ability of renal organoids to undergo nephrogenesis upon Wnt/ β -catenin pathway—mediated tubule induction with a GSK-3 inhibitor (BIO) or by initiation through the ureteric bud (UB). We found that 5000 cells of MM cells are necessary to successfully form renal organoids with well-structured nephrons as judged by fluorescent microscopy, transmission electron microscopy (TEM), and quantitative Polymerase Chain Reaction (qPCR). These mouse organoids also recapitulated renal secretion function in the proximal tubules.

Conclusions: We show that a significant decrease of cells used to generate renal mouse organoids in a dissociation/re-aggregation assay, does not interfere with development, and goes toward 3Rs. This enables generation of more experimental samples with one mouse litter, limiting the number of animals used for studies.

KEYWORDS

3Rs, dissociation/re-aggregation assay, kidney development, minimal cell number, renal organoids

1 | INTRODUCTION

During normal embryogenesis, kidney development occurs as a result of cross-talk between the ureteric

bud (UB) and the metanephric mesenchyme (MM) cells. Their interaction triggers a signaling cascade, which induces nephrogenesis and leads to nephron formation.

This is an open access article under the terms of the Creative Commons Attribution-NonCommercial-NoDerivs License, which permits use and distribution in any medium, provided the original work is properly cited, the use is non-commercial and no modifications or adaptations are made.

© 2021 The Authors. *Developmental Dynamics* published by Wiley Periodicals LLC on behalf of American Association for Anatomy.

During renal development, the UB outgrows from the Wolffian duct and invades the MM. The first contact of MM and UB leads to induction of the MM cells, which form condensed MM caps around UB tips and later the renal vesicles. These vesicles develop into comma- and S-shaped bodies, which elongate and develop into nephrons consisting of a glomerulus, proximal tubule, loop of Henle and distal tubules connected by a collecting duct system.¹ Kidneys are, however, quite autonomous and self-developing even outside of an embryo body.^{2,4} When cultured *in vitro*, kidneys develop appropriately structured nephrons that are connected with the collecting duct system.⁵ Even upon dissociation and re-aggregation, the kidneys are able to self-organize and generate renal organoids that resemble the *in vivo* organ with only small noticeable difference that instead of one collecting duct system, a network of disperse collecting ducts occurs.^{3,6,7}

Some organoids, such as the “mini guts” or “mini livers” can be generated from single cells, namely the intestinal tract stem/progenitor cell expressing *Lgr5*.^{8,9} However, unlike intestinal or liver tissue, the kidneys do not contain a single stem cell population as they develop from reciprocal interaction of two different populations of cells: epithelial—the UB and mesenchymal—the MM. The MM is quite heterogenous cell mixture containing nephron progenitors,^{10,11} stromal cells,^{12,13} and endothelial progenitors¹⁴ where FGFs, BMPs, and Wnts maintain the balance between cell-renewal and differentiation.¹⁵ While the UB can be removed from kidney culture and successfully replaced by BIO (6-Bromindirubin-3'-oxime)¹⁶ or LiCl,¹⁴ stromal and nephron progenitors within the MM are required for appropriate kidney development.¹⁷

The organoids from primary renal cells have already been used to generate chimeric cultures, in cases when the *in vivo* gene knock out is leading to early lethality,³ or is difficult to study,¹⁸ or to reduce time and cost of chimeric animals generations.^{7,19} However, all above-mentioned studies used a quite high number of cells. In this paper, we aimed to define a minimal number of cells required for formation of morphologically and functionally accurate *in vitro* kidney organoid cultures. We systematically evaluated kidney organoid formation and development of renal structures within the context of their size and we experimentally derived the minimal essential number of cells required for successful generation of renal organoids. This study is of particular importance, since the cellular number is known to be crucial parameter governing the tissue differentiation processes during the embryogenesis.²⁰ Moreover, since we studied primary cells, this work may help scientist studying development to reduce the number of animals used, since smaller number of cells required for organoid generation will significantly reduce the number of animals used,

which goes well with the 3Rs: reduction, replacement, refinement.

2 | RESULTS

Renal organoids generated from primary cells contained from 80 000 to 180 000 cells^{3,7} which gave rise to several nephrons. In this manuscript, we attempted to establish the lowest number of primary cells necessary to generate renal organoids containing nephrons.

2.1 | Successful organoid formation required to reach a minimal cell number

We calculated that the E11.5 mouse kidney rudiments contained on average 20 000 cells of which about 15 000 were MM cells and 5000 were UB cells (Figure 1A). Interestingly, kidney rudiments presented a large variation in size as some litters had visually smaller kidney rudiments than others, although they were staged using the fetus characteristic and somite counts (44–48 somites).²¹ This variation was represented in the cell counts after dissociation, as the smallest counted kidney rudiments consisted of 15 000 cells while the largest had almost twice the numbers of cells (26 000 cells) (Figure 1B). The same was true for the MM cells, for which we counted from 10 000 to 26 000 cells per kidney rudiment (Figure 1B). Interestingly, the number of UB cells per kidney rudiment was more conserved, ranging from 4300 to 6300 cells per kidney rudiment (Figure 1B). Therefore, on average, the kidney rudiment consisted of 75% of the MM cells and 25% of the UB cells (Figure 1C). We therefore generated organoids from limited number of MM cells: 30 000, 15 000, 10 000, 5000, and 2500 using a traditional centrifuge method and an air-medium interface culture system.^{3,14} We then tested whether the organoids were able to generate nephrons. We depleted the MM of the natural inducer tissue, the UB, and induced nephrogenesis using small molecule BIO (6-Bromindirubin-3'-oxime, 5 μ M) instead. BIO is known inhibitor of GSK-3 and acts as an efficient (stronger than UB²) inducer of nephrogenesis¹⁶; it stabilizes β -catenin in the cytoplasm and allows its translocation into the nucleus, where it coordinates the transcription of specific genes. The viability of the MM cells after dissociation into single cell suspension was >90%, and all samples generated viable cell aggregates/spheres (Figure 2 A,B). Viability tests performed at days 1 and 3 of organoid culture showed that majority of cells which did not become induced by day 3, in all organoid samples, were undergoing apoptosis (Figure 2B) as depicted by PI staining. In samples consisting of 30 000,

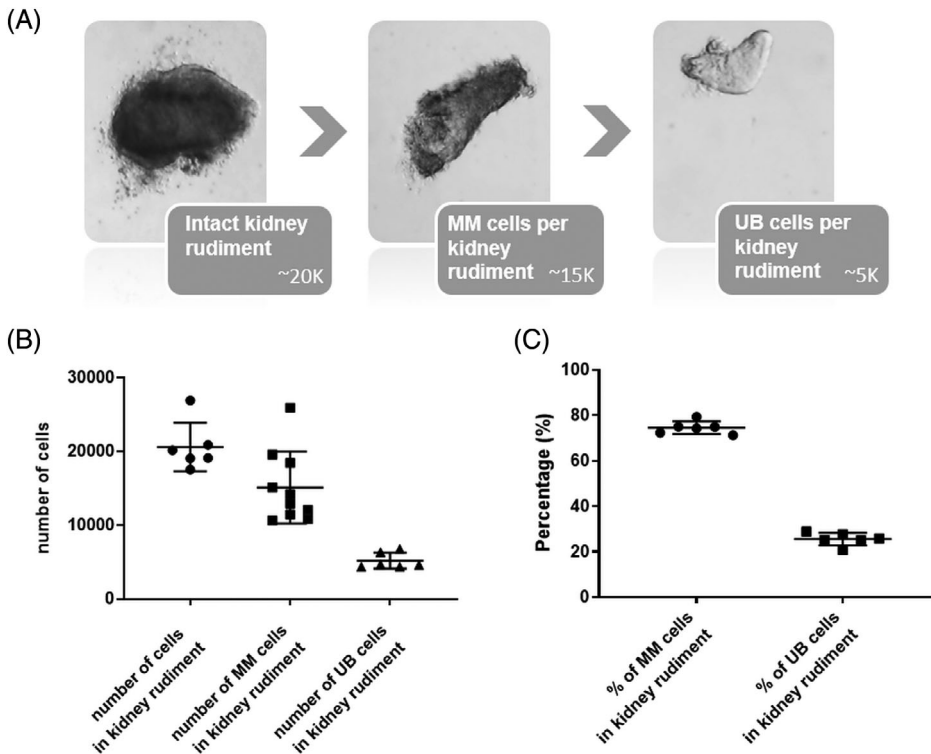


FIGURE 1 Composition of kidney rudiments. (A) Schematic presenting components of the E11.5 embryonic kidneys, (B) Graph presenting number of counted kidney cells in the whole kidney (circle marks), metanephric mesenchyme (MM) compartment (square marks) and ureteric bud (UB) compartment (triangle marks) mean \pm SEM, (C) Graph presenting percentage that the MM and UB cells represented in the whole kidney rudiment; mean \pm SEM

15 000, 10 000, and 5000 the PI-positive cells, undergoing apoptosis located mainly to the outer area of the organoids, and only in few places inside the organoids. Similar observation was done in intact MM (iMM) cultured for 3 days with the difference that the outer cells were healthy (Figure 2E). This difference may be explained by lack of dissociation step in the latter samples, therefore supporting cell survival, although some dying cells were also observed in the intact kidney (iKidney) cultures (Figure 2F). The 2500 cells organoids presented high level of apoptosis and renal structures did not develop by day 6 of culture (Figure 2B-D).

We further analyzed organoids grown for 3 days by measuring the total area of organoids and that of translucent spots, which are indicators of developing renal vesicles on a bright field images (Figure 2 C,D,G). We found that organoids smaller than those generated by 5000 cells were not induced by BIO and failed to form nephrons. We compared it to iKidney and iMM cultured with and without BIO induction and showed that the uninduced iMM (-BIO) did not undergo tubulogenesis and similarly to 2500-cell organoids failed at development of renal structures (Figure 2 E,F). We further analyzed organoids cultured for 3 days by immunostaining with laminin to confirm the number of renal vesicles forming in each aggregate (Figure 2D). Based on these studies, we can conclude that the size of the organoid correlated well with the number of developing nephrons and the induced area (Figure 2G), while lack of induction by day 3 led to apoptosis of the MM cells.

To ask whether the MM cells would behave similarly when induced with natural inducer, the UB, we tested two organoid variants: we dissociated whole kidney rudiments at E11.5, counted the cells and generated organoids (i) containing 30 000, 15 000, 10 000, 5000, and 2500 cells, and (ii) where we increased the size of organoids by 25% to account for the UB population. We observed that in all cases the cells generated viable and compact spheres at day 1 (Figures 3A and 4A). However, by day 3 in the first variant, the organoids formed by 5000 and 2500 cells had more apoptotic cells and presented lack of tubulogenesis as depicted by immunofluorescent staining of day 6 organoids with absence of epithelialization (Figure 3B,C). On the other hand, in the second variant, all organoids presented good viability even at day 3 of culture. However, the 2500 organoids did not survive to day 6 and remained uninduced, leading to lack of epithelial structure formation (Figure 4 B,C). In both variants, the organoids that underwent tubulogenesis presented expression of renal markers similar to the one observed in iKidneys (Figure 5C). Thus suggesting, that the number of MM cells is more important than the overall number of cells.

2.2 | Small organoids generated nephrons containing all segments

In order to establish whether the organoids were able to generate well-structured nephrons from a limited number

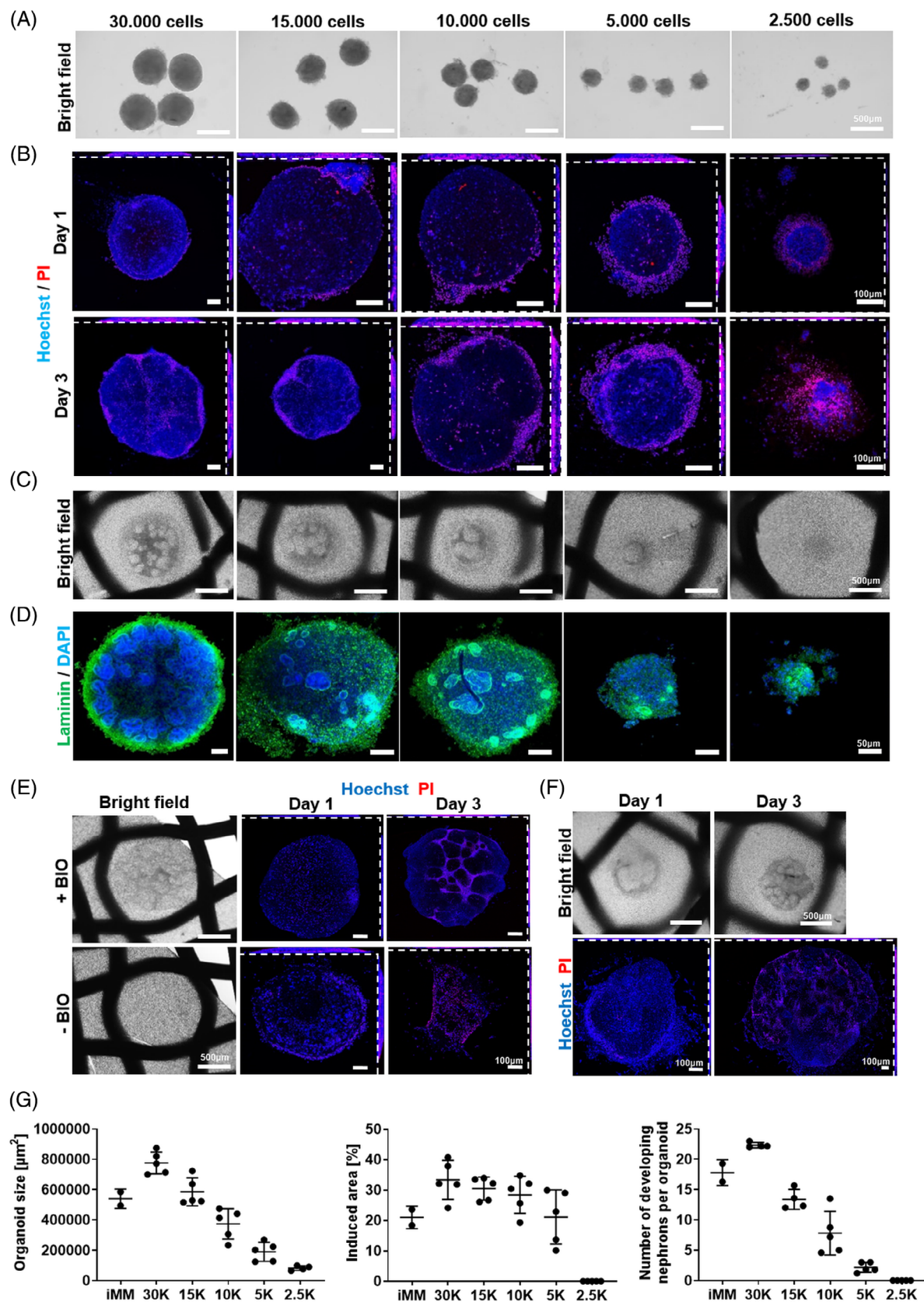


FIGURE 2 Legend on next page.

of cells, we analyzed the expression patterns of renal markers in the organoids. A series of immunostainings and quantitative Polymerase Chain Reaction (qPCR) analyses showed that all organoids, except for those ones generated from 2500 cells, formed nephrons containing the distal tubules (Figure 5; Pax2, Slc12a1), proximal tubules (Figure 5; LTL, Aqp1, Slc4a4), and glomeruli (Figure 5; Wt1, Synpo, Podocin) at day 6 of culture. Although there were no significant changes in gene expression between the organoids samples, a trend could be observed: the smaller the organoid, the lower the expression level. The gene expression in iMM presented similar level to same genes expression observed in organoids generated by 15 000 and 10 000-cells organoids.

We then continued to analyze the ultrastructure of generated organoids (Figures 6 and 7). Transmission electron microscopy (TEM) analysis of samples cultured for 6 days showed that in organoids sizes 5000 to 30 000, glomeruli-like structures could be observed (Figures 6A and 7A,B). The glomeruli presented as round aggregates of cells surrounded with a basement membrane. The developing podocytes (P) were connected with each other with tight junctions and junctional complexes and were forming primary foot processes (in all organoid sizes). Moreover, in 15 000 and 30 000 organoids, a layer of flattened cells, which could represent the parietal epithelial cells (PEC) of putative Bowman's capsule, surrounded the podocyte clusters (Figure 6A,B). Furthermore, we studied the degree of tubulogenesis in organoids. We identified a set of tubules, which at day 6 or 8 of development did not have an open lumen, but possibly three different kinds of tubules were observed (Figures 6C-H and 7C-G): developing proximal tubules, distal tubules and the loops of Henle. The tubular cells with numerous tight junctions and junctional complexes, and a very rich vacuolar apparatus at the apical site represented developing proximal tubules; there was no obvious brush border at this point of development, although in some cases microvilli-like structures were observed (Figure 6C,D). The second type of tubules was the only one with lumen,

and due to a small tubule diameter and presence of flattened cells connected with tight junctions at the apical surface, we believe, they may represent the loops of Henle (Figure 6E,F). The third set of tubules, which may represent the developing distal tubules had cells tightly connected with each other by numerous infoldings of cell membrane along the lateral site of the cells, had elongated mitochondria and did not have so many vacuoles at the apical site (Figure 6G,H). The smallest organoids generated from 2500 cells were represented by clusters of cells, which were undergoing apoptosis, and were devoid of any structures (Figures 2 B-D and 6I,J).

2.3 | Small organoids presented proximal tubule functionality but were delayed in development

Since all organoid sizes, except for the 2500-cell organoid, presented development of fully structured nephrons, we asked if these nephrons were functional. One of the functions of the kidney is to remove metabolic waste. A large family of membrane transporters Slc 22, known as well as organic anion transporters (Oat's), may be efficiently and specifically blocked by probenecid (Figure 8A,B). We therefore used Oats activity to test the renal secretion function in generated organoids.

At day 6 of development, the iKidney and iMM samples had an active uptake of 6-carboxyfluorescein (6-CF, 10 μ M) from the solution, and the uptake was efficiently blocked by probenecid (200 μ M, CTRL).⁷ We immediately imaged the organoid samples and analyzed the intensity of 6-CF fluorescence in the cells (Figure 8 B). The 6-CF up-take and its secretion were similar between iKidney and iMM with regards to fluorescent intensity and were observed at day six of culture also in 10 000, 15 000 and 30 000- cell organoids (Figure 8B,C). The uptake of 6-CF in 5000-cell organoids at day six of culture was not different from control samples. We concluded that the secretory function of proximal tubules in

FIGURE 2 Generation of renal organoids of various sizes. (A) Bright field images of generated spheres of renal organoids using 30 000, 15 000, 10 000, 5000, and 2500 cells before they were placed into Trowel culture system; scale bar—500 μ m. (B) Viability staining of propidium iodine and Hoechst of renal organoids performed at day 1 (upper panel) and day 3 (lower panel) of culture; maximum intensity projections (MIPs) and cross-sectional views, scale bar—100 μ m. (C) Brightfield images of generated renal organoids in a Trowel culture at day 3; scale bar—500 μ m. (D) Immunofluorescent images of generated renal organoids at day 3 of culture with Laminin (green) and DAPI (blue) depicting the presence of renal vesicles or renal tubules in the samples; MIPs were used to generate the shown images; scale bar 50 μ m. (E) Bright field images at day 3 of culture (left); scale bar - 500 μ m; and viability staining (right) at days 1 and 3 of culture in intact metanephric mesenchyme samples induced with BIO (+BIO) and without induction (-BIO); scale bar 100 μ m, (F) Bright field images of intact kidney cultured for 1 and 3 days (upper panel); scale bar—500 μ m, and viability staining of days 1 and 3 intact kidney samples (bottom panel), scale bar—100 μ m, (G) Analysis of the organoids: the size, induced area and number of developing nephrons (number of experiments—2-5, number of samples analyzed per experiment—20)

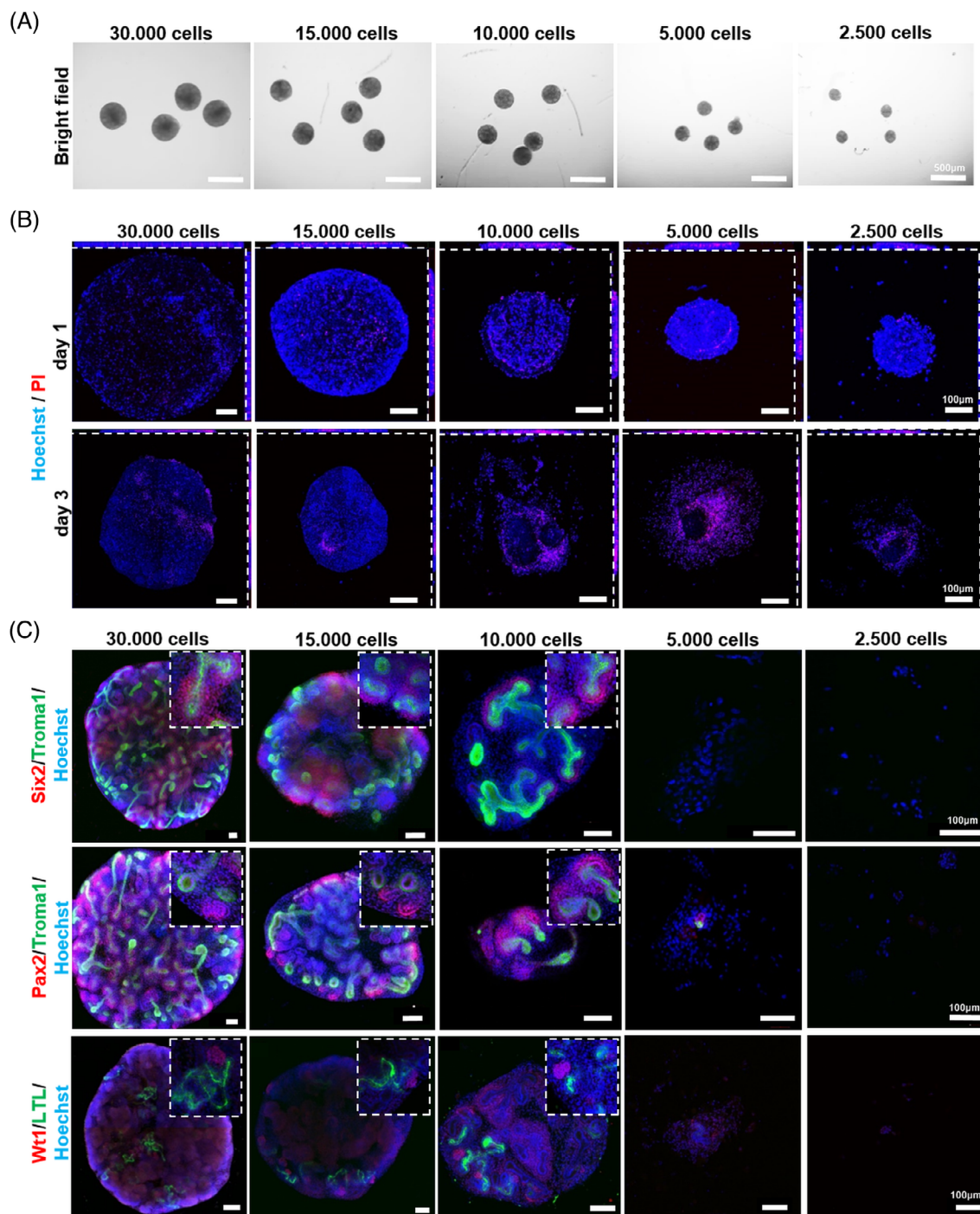


FIGURE 3 Generation of ureteric bud (UB)-induced organoids of various sizes. (A) Brightfield images of generated spheres of renal organoids (MM + UB) using 30 000, 15 000, 10 000, 5000, and 2500 cells before they were placed into Trowel culture system; scale bar—500 μm . (B) PI and Hoechst staining of renal organoids presenting viable aggregates of cells at day 1 of culture (1 hour after transfer of spheres into Trowel culture), and at day 3 of culture, where 5000 and 2500 organoids did present increased number of apoptotic cells (PI+) at day 3; maximum intensity projections (MIP) and cross-sectional views were used to generate presented images, scale bar—100 μm . (C) immunofluorescent confocal images of day 6 organoids presenting: ureteric bud structures (Troma1) surrounded with nephron progenitors (Six2)—upper panel, ureteric bud (Troma1) and nephron progenitors as well as developing nephrons (Pax2)—middle panel, and the development of early glomeruli (Wt1) and proximal tubules (LTL)—bottom panel. Out of all samples the development was not observed in organoids generated by 5000 and 2500 cells

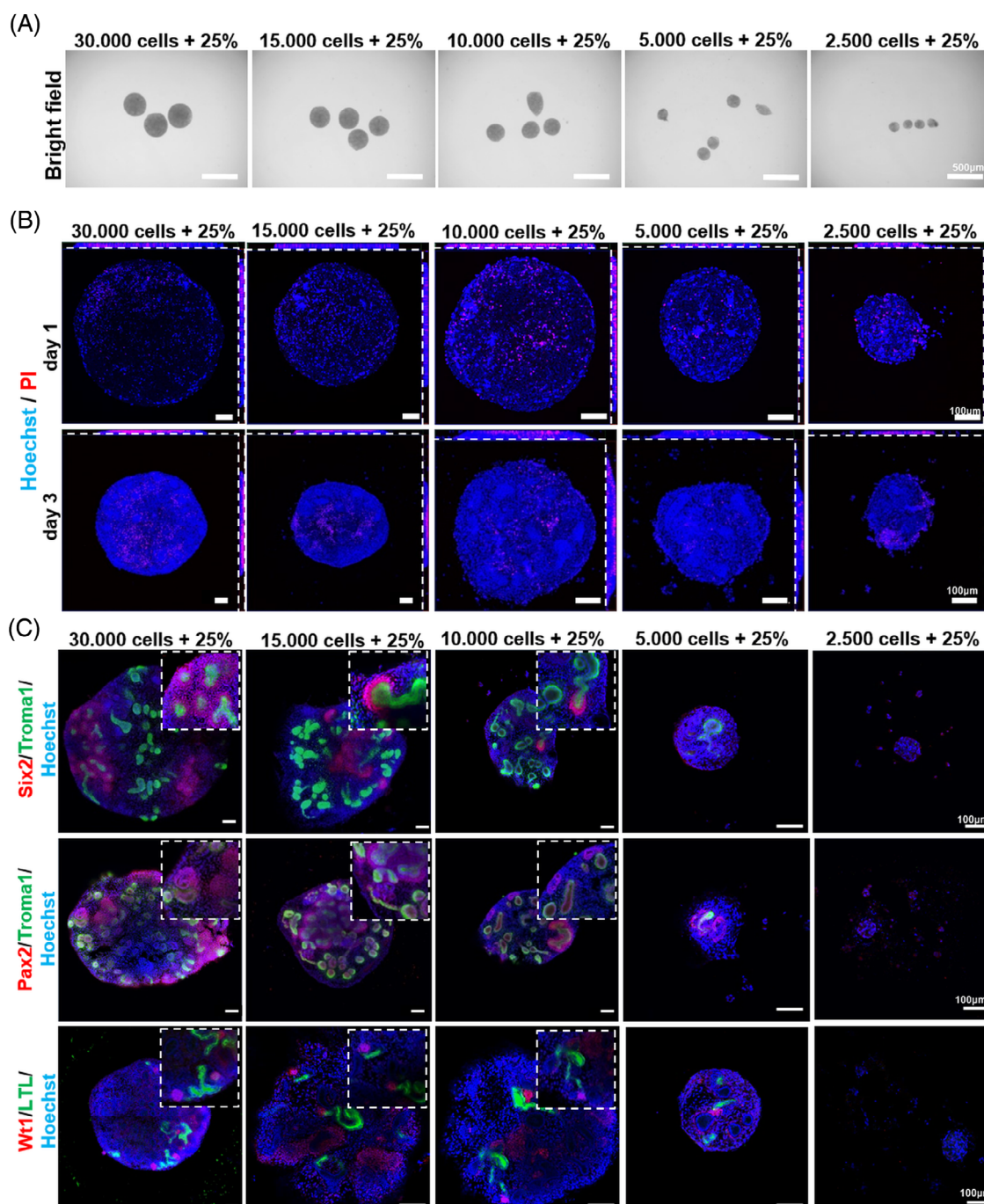


FIGURE 4 Generation of ureteric bud (UB)-induced organoids of various sizes with 25% of cells more. (A) Bright field images of generated spheres of renal organoids (MM + UB) using 30 000, 15 000, 10 000, 5000 and 2500 plus 25% of cells before they were placed into Trowel culture system; scale bar—500 μm. (B) PI and Hoechst staining of renal organoids presenting viable aggregates of cells at day 1 of culture (1 hour after transfer of spheres into Trowel culture), and at day 3 of culture, all organoids present good viability at day 3; maximum intensity projections (MIP) and cross-sectional views were used to generate presented images, scale bar—100 μm. (C) immunofluorescent confocal images of day 6 organoids presenting: ureteric bud structures (Troma1) surrounded with nephron progenitors (Six2)—upper panel, ureteric bud structures (Troma1) and nephron progenitors as well as developing nephrons (Pax2)—middle panel, the development of early glomeruli (Wt1) and proximal tubules (LTL)—bottom panel. Out of all samples, the development was not observed in organoids generated by 2.5 K cells

5,000-cell organoids was not present at this time point. However, at day 11 of culture, a low level of secretory function was observed. Although this activity in the 5000

cell organoids was weaker than in the 10 000-cell organoids at day six, the difference was not significant (Figure 8D [marked with #]). This data suggests that

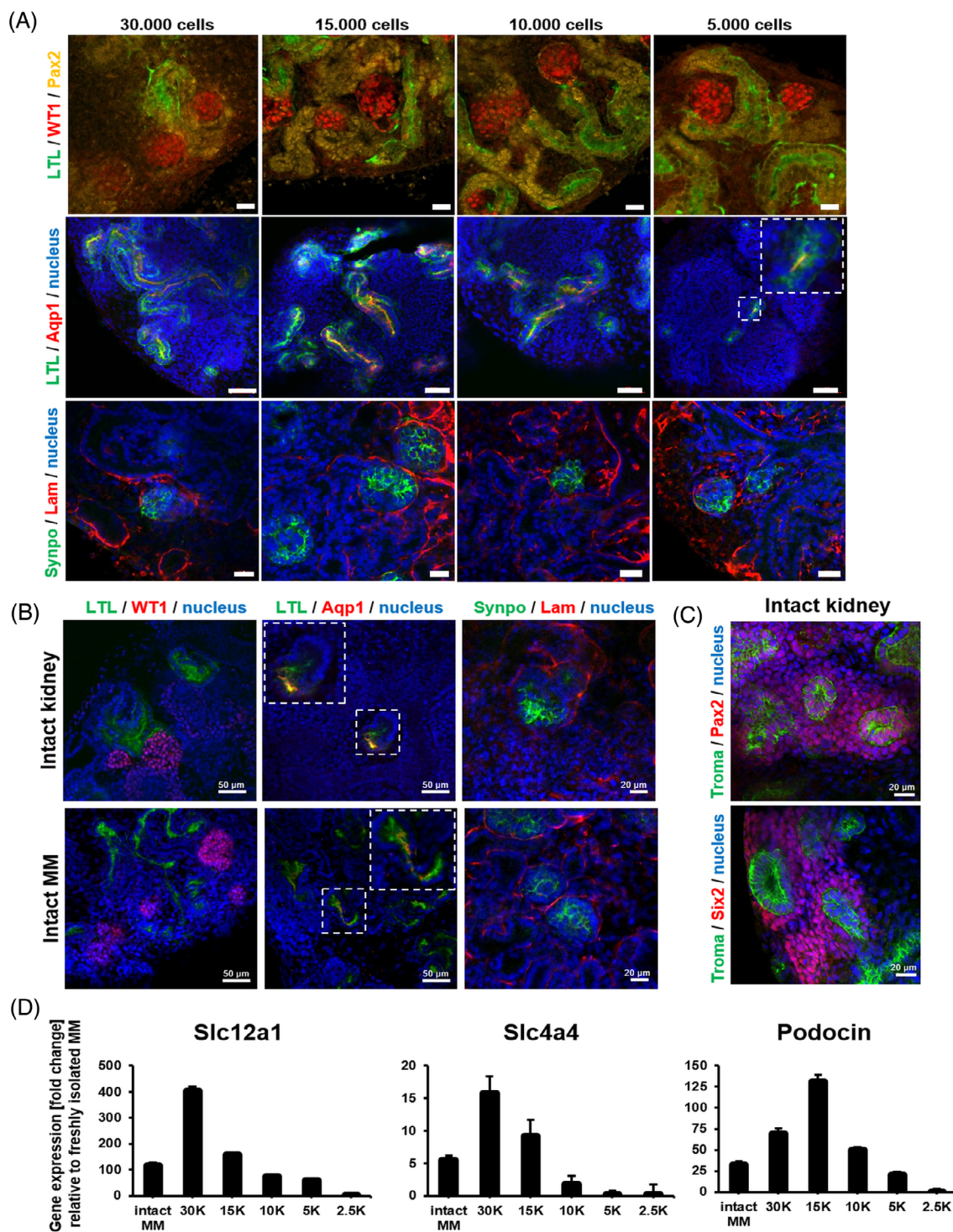


FIGURE 5 All sizes of organoids generated nephrons containing all segments at day 6 of culture. (A) Upper panel: immunostaining depicting connection between glomeruli (WT1+) and proximal tubules (LTL+) and presence of distal tubules (Pax2 + LTL-); (upper panel) scale bar 20 μ m. Middle panel: immunostaining depicting presence of proximal tubules (LTL+) with water channels present (Aqp1); scale bar 50 μ m. Bottom panel: immunostaining presenting glomeruli (Synpo+) surrounded with basement membrane (Laminin+) in generated organoids; scale bar 20 μ m. (B) Immunostaining of intact kidney samples (upper panel) and intact metanephric mesenchyme (bottom panel) presenting connection between glomeruli (Wt1+) and proximal tubules (LTL+), co-expression of LTL and Aqp1 in proximal tubules; scale bar—50 μ m, and glomeruli (Synpo+) surrounded with basement membrane (Laminin+); scale bar—20 μ m, (C) Immunostaining of intact kidney samples presenting expression of Pax2 and Six2 alongside the ureteric bud marker—Troma1, (D) Graphs presenting qPCR analysis of genes expression in developing organoids; distal tubule—Slc12a1, Proximal tubule—Slc4a4 and glomeruli—Podocin; (number of experiments—3; number of samples pooled per each organoid size—10–20, Mean \pm SEM)

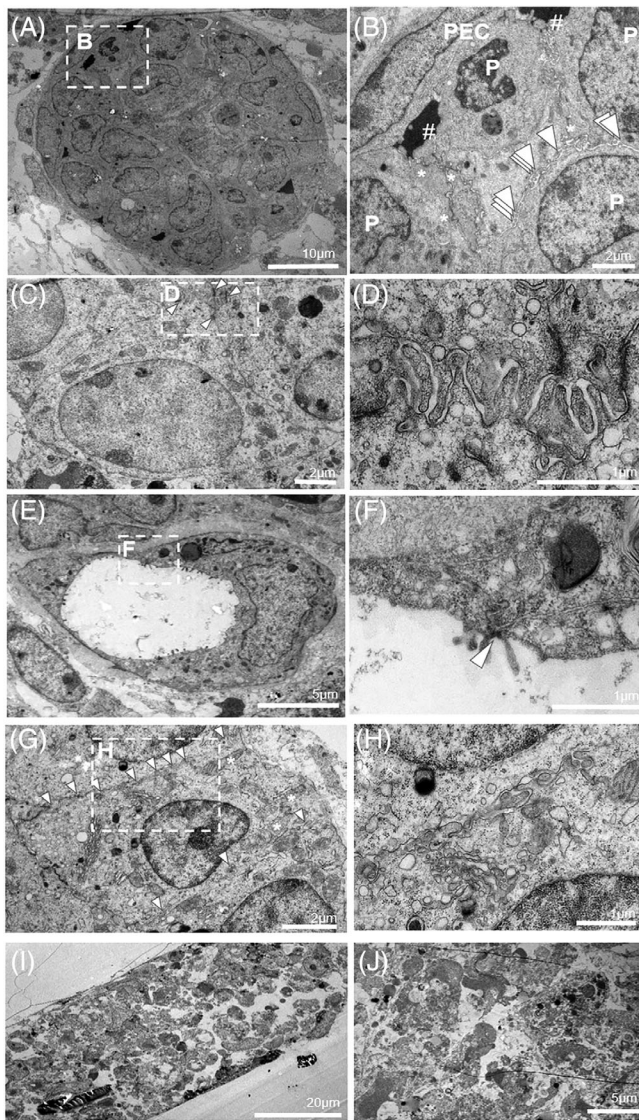


FIGURE 6 Ultrastructure of developing organoids. (A) Glomerulus, (B) Glomerulus, P-podocyte, PEC, parietal epithelial cell, arrowhead, foot processes, star, tight junctions, hash, putative urinary space, (C) Proximal tubule, arrowheads, tight junctions, (D) Proximal tubule developing brush border, (E) Loop of Henle, (F) Loop of Henle tight junctions between cells, (G) Distal tubule, arrowheads, cell membrane infoldings; star, elongated mitochondria, (H) Distal tubule lateral site presenting basement membrane infoldings, (I) Lack of renal structures in organoid generated from 2500 cells, (J) Lack of structures in organoid generated with 2500 cells

there is a delay in development of the smallest organoids. The qPCR data of *Oat1* and *Oat3* expression in organoids presented no significant changes between samples, but again, a trend could be observed; the smaller the organoid, the lower the gene expression (Figure 8E). However, the level of *Oat1* and *Oat3* expression in iMM was placed somewhere between 10 000 and 5000-cell organoids whereas the functionality was high, similar to

iKidney. This might be explained, by development of proximal tubules with fewer but highly active transporters (Figure 8D,E).

3 | DISCUSSION

During embryogenesis, reaching a specific cell number threshold regulates progression from one developmental stage to next. For example, in order to proceed to gastrulation phase, a mouse embryo needs to reach approximately 1000 cells, and smaller zygotes experience delay in development until the required number of cells, is reached.²⁰ In this report, we investigated the minimal number of cells required to generate functional renal organoids. Our data show that induction with BIO resulted in 100% induction rate in all organoid samples but the 2500-cell organoid, which showed no induction at all (Table 1). Neither increasing the speed of centrifugation (from 1380g to 1450g) nor elongation of centrifugation time (from 20 to 30 minutes) improved the tubulogenesis in the 2500-cell organoids. It is worth noting that the original centrifugation time of 2 minutes³ generated spheres from more than 15 000 cells, while using less cells resulted in lack of aggregates that would undergo nephrogenesis (data not shown). Therefore, from experiments, in which we induced the MM with BIO, we concluded that the minimal number of cells to generate renal organoid is 5000 cells. However, from the experiments, where we induced the MM with UB cells, we saw, that not the overall number of cells is important, but the cells' origin. When we generated organoids from 5000 cells of UB and MM origin, they did not develop nephrons, the tubulogenesis did not start and they were undergoing apoptosis. Yet, when we increased the size of the organoid to keep the number of MM cells at 5000 and added more cells to account for the UB (25%), they were developing in a similar manner as those induced by BIO. Therefore, the minimal number of cells to generate renal organoid containing nephrons is 5000 of MM cells. Indeed, nephron ablation studies showed that upon removal of 40% of the *Gdnf*-expressing cells, kidneys are significantly smaller and develop less glomeruli.²² In this study,²² the limits of cells for renal agenesis was not investigated, and given our results, the ablation would have to exceed 66.6% of MM cells for that to happen.

We generated different sizes of renal organoids from primary MM cells and analyzed their development. While our immunofluorescence and TEM data suggested that all generated organoids underwent nephrogenesis and generated nephrons with evidence of early segmentation after 6 days in culture, qPCR data of genes expression

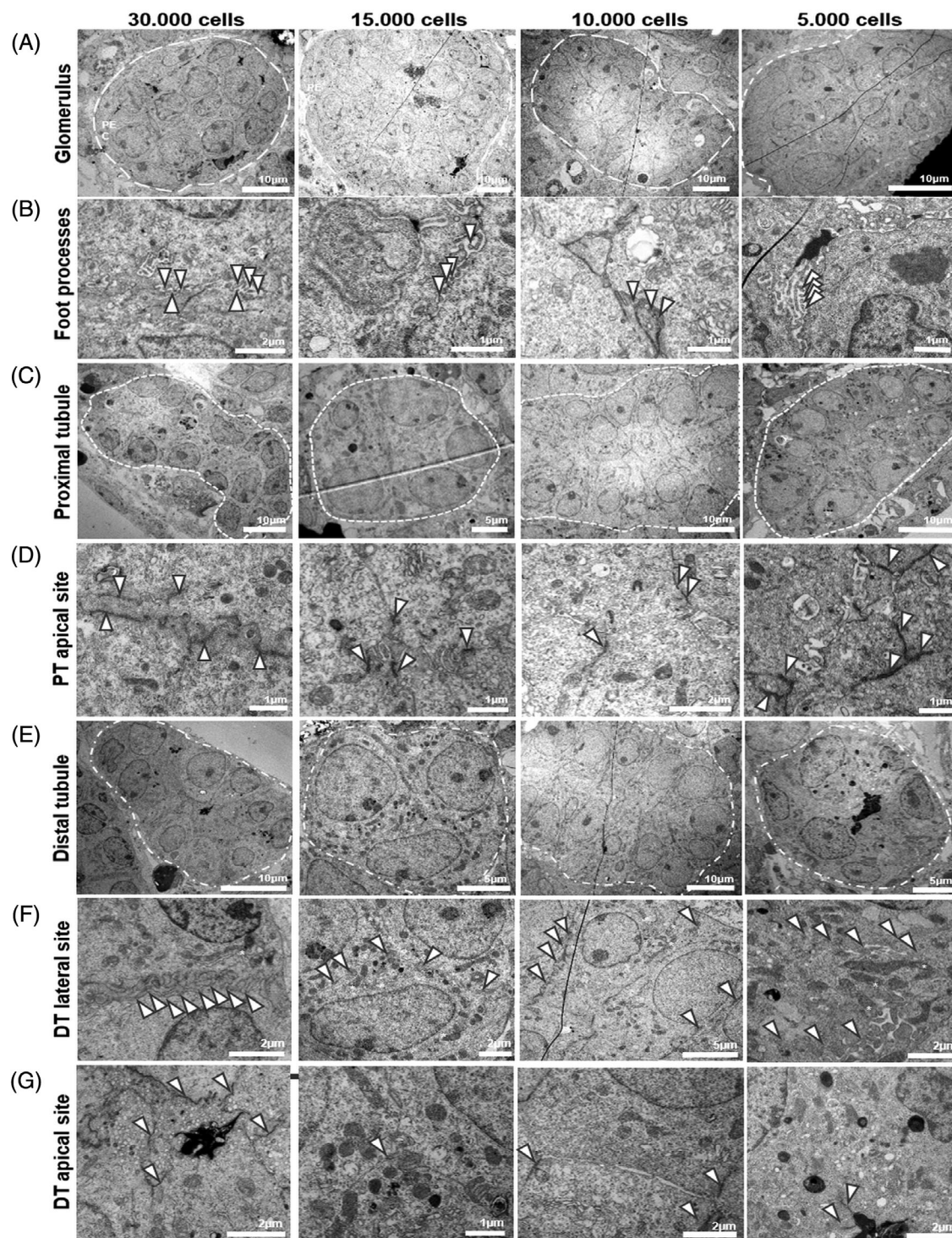


FIGURE 7 Ultrastructure of developing organoids. (A) Glomerulus, in some cases contain parietal epithelial cells (PEC) surrounding the podocytes, (B) Developing foot processes between podocyte cells, marked with arrowheads, (C) Proximal tubules, (D) Apical site of proximal tubule presenting rich vacuolar apparatus, (E) Distal tubule, (F) Lateral site of distal tubule presenting basement membrane infoldings marked with arrowheads and elongated mitochondria marked with stars, (G) Apical site of distal tubule presenting not so rich vacuolar apparatus, tight junctions marked with arrowheads

specific for each nephron section suggested that smaller organoids had lower gene expression (Figure 5). These data, together with our analysis of organoid proximal

tubular cells functionality (Figure 8) indicated that the small organoids were delayed in development. This data stays in agreement with observations of whole embryo

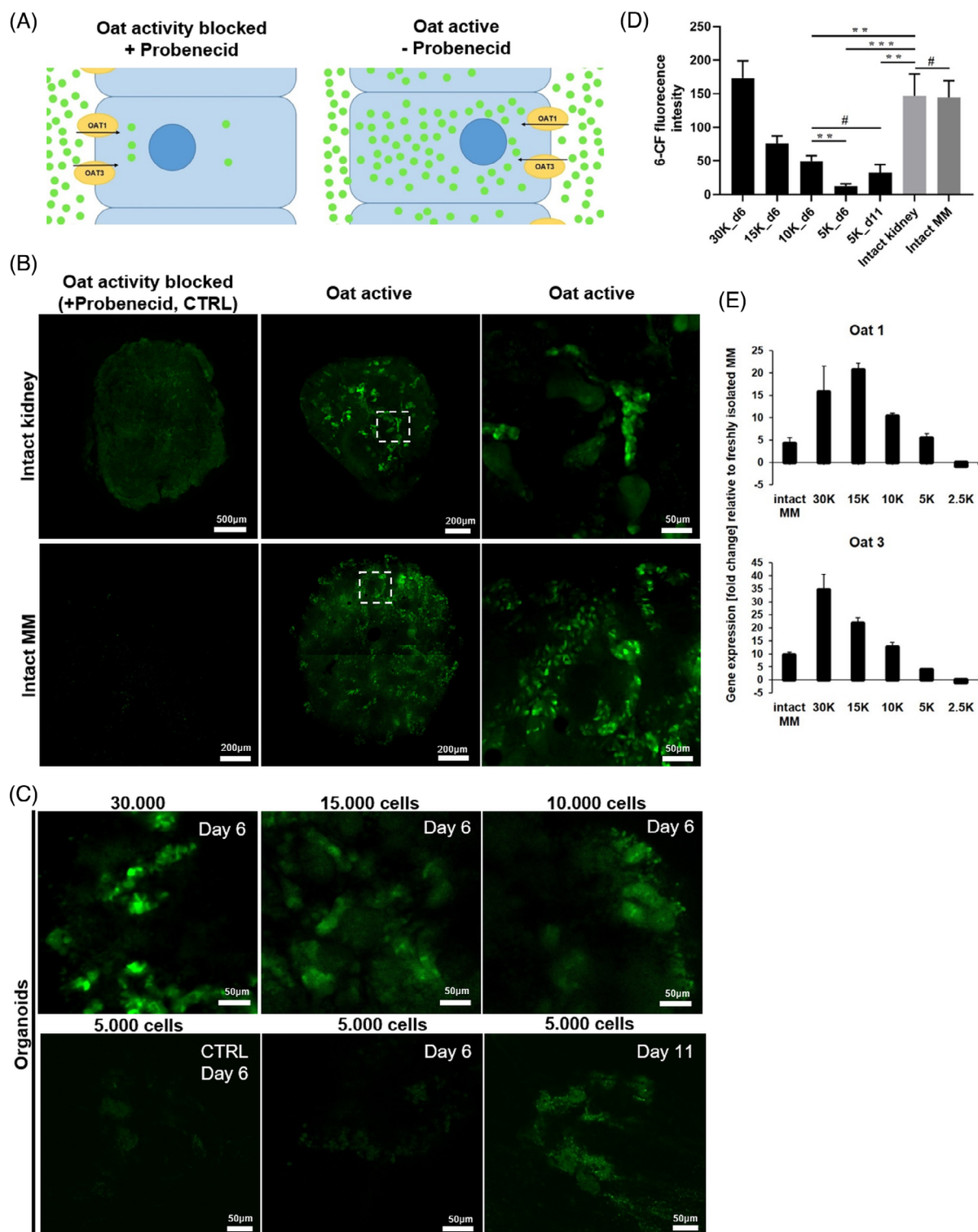


FIGURE 8 Organoids have Oat activity. (A) Schematic presenting activity of Oat1 and Oat3 in proximal tubule cells. On the left, the activity of Oat1 and Oat3 was blocked with probenecid, while on the right, the Oat1 and Oat3 actively transport the small molecule of 6-carboxyfluorescein (6-CF, green) into the cell, (B) confocal image of intact kidney (upper panel) and intact metanephric mesenchyme (bottom panel) samples cultured for 6 days where the up-take of 6-CF was inhibited by probenecid (CTRL), and Oats activity presenting up-take of 6-CF, (C) secretion function in 30 000, 15 000, and 10 000 organoids at day 6 of development (upper panel), and secretion function in 5000 organoid at days 6 and 11 of development (bottom panel), (D) 6-CF fluorescence intensity profile, *** $P < 0.0001$, ** $P < 0.001$, # not significant, (E) qPCR graph depicting presence of Oat1 and Oat3 in developing organoids

TABLE 1 Induction rate of renal organoids

	EXP 1	EXP 2	EXP 3	EXP 4	EXP 5	Total	%
30 K	3/3	3/3	3/3	5/5	5/5	19/19	100
15 K	3/3	3/3	3/3	5/5	5/5	19/19	100
10 K	4/4	4/4	5/5	5/5	5/5	23/23	100
5 K	4/4	4/4	5/5	6/6	6/6	25/25	100
2.5 K	—	0/5	0/5	0/4	0/4	0/18	0

development, where reaching a certain number of cells allows progression to next milestone.

The bottom limit of cells that are able to generate functional renal organoids might be placed somewhere between 5000 and 2500, as may be suggested by recent work²³ where the iPSC-derived renal organoids were three-dimensional (3D) bioprinted by using as little as 4000 cells. We have used FACS to sort specific number of MM cells (5000, 4000, 3000, 2500) however, the cells did not survive well the sorting procedure and none of the pellets generated spheres (data not shown).

10K renal organoids were generated from hiPSC in a recent study by Boreström, and after 25 days of culture they were not different from 100K organoids (RNA-seq analysis), although an earlier time point was not investigated.²⁴ There are two possibilities: (i) iPSC behave differently to primary cells in respect to cell number, and (ii) that the smaller organoids do require longer culture time to reach a similar level of maturity as bigger organoids, which was suggested by a functionality assay in the current study. Nevertheless, it should be kept in mind, especially in generating organoids for drug-related toxicity screens that an appropriate number of cells is used, and generated organoids are fully functional in order to avoid false-negative/false-positive results.

To summarize, the ability to generate small functional renal organoids from primary cells is in accordance with the 3Rs rule: reduction, replacement, and refinement. Reduction of number of cells required for renal organoid formation means that more samples can be prepared from one mouse litter, substantially reducing the number of animals used. Moreover, while large organoids may be required for transplantation studies those small in size might do better in 3D bioprinting or microfluidic set-ups.

4 | EXPERIMENTAL PROCEDURES

4.1 | Ethical statement

The animal care and experimental procedures in this study were performed in accordance with the Finnish national legislation on the use of the laboratory animals,

the European Convention for the protection of vertebrate animals used for the experimental purposes (ETS 123), and the EU directive 86/609/EEC. The animal experimentation was also authorized by the Finnish National Animal Experiment Board (ELLA) as being compliant with the EU guidelines for animal research and welfare.

4.2 | Animals and cells

The embryos for this study were obtained from pregnant wild-type CD-1 mice. The metanephric kidneys were dissected from embryonic day (E) 11.5 mouse embryos in chilled Dulbecco's phosphate-buffered saline (PBS) buffer (Sigma, Darmstadt, Germany). Following a 30 seconds incubation in pancreatin (Sigma)/trypsin (Sigma) (1.125%/2.25%) solution, the MM was mechanically separated from the UB.²⁵

The MM was incubated in 0.1% BSA (Sigma) in PBS and Collagenase IV (Worthington, Columbus, OH, USA) for 10 to 15 minutes at 37°C. The MM was pipetted twice to help with cell separation and once the single cells were identified down the microscope, the reaction was stopped using kidney culture medium (DMEM (#21885-025, ThermoFisher Scientific, Waltham, MA, USA) supplemented with 1% (v/v) Penicillin/Streptomycin (Sigma) and 10% (v/v) FBS (Gibco, Waltham, MA, USA)). The single MM cells were washed three times in kidney medium and cell number was counted using TC20 Automated Cell counter (Bio-Rad, Hercules, CA, USA).

The UB cells were incubated in 1× trypsin/EDTA solution for 10 minutes at 37°C; samples were vigorously pipetted after 5 minutes of incubation, in order to generate single cell solution. Following the incubation time, cells were washed three times with kidney culture medium and the number of cells was counted using TC20 Automated Cell counter (Bio-Rad).

For induction with UB, whole kidneys were treated with 1X trypsin/EDTA solution for 10 minutes at 37°C. Samples were pipetted vigorously after 5 minutes of incubation. Upon identification of single cells, the trypsinization was stopped by adding equal volume of complete kidney culture medium. The single renal cells were washed three times in kidney medium and cell number was counted using TC20 Automated Cell counter (Bio-Rad).

4.3 | Organoid generation

Following cell counting, an appropriate amount of media with cells (30 000, 15 000, 10 000, 5000, 2 500) were transferred into low binding tubes (Eppendorf, Hamburg, Germany) and the GSK-3 inhibitor (BIO) (Sigma, #B1686; 5 μ M) was added. Tubes with cells were centrifuged at 1380 \times g for 20 minutes and transferred in an incubator for overnight incubation at 37°C. The next day, the pellets were transferred onto Millipore filters (1 μ m; Whatman, Maidstone, UK) and cultured in fresh kidney culture medium at 37°C.^{18,25} Medium was changed every 2 to 3 days.

When induction with UB was set up, an appropriate number of cells in kidney culture medium were transferred to low binding tubes and the ROCK inhibitor (Y-27632) (#1254, 10 μ M, Tocris, Bristol, UK) was added for 24 hours of culture.³ Tubes with cells were centrifuged at 1380 \times g for 20 minutes and transferred into the incubator for ON incubation at 37°C. On the next day, the pellets were transferred onto Millipore filters (1 μ m; Whatman) and cultured in fresh kidney culture medium at 37°C.²⁵ Medium was changed every 2 to 3 days.

4.4 | Viability staining

In order to investigate the viability of the samples and assess the incidence of apoptosis, we used propidium iodide, PI (#P1304MP, Invitrogen, Waltham, MA, USA) and Hoechst 33342 (Thermo Scientific, #H1399) nucleic acid stains. The Hoechst stains all cells, while PI is membrane impermeant and excluded from viable cells. The Hoechst and PI were added to the culture medium in a dilution of 1:1000 for 40 minutes incubation in the incubator at 37°C and 5% CO₂. Following this time, samples were briefly washed 2 \times with PBS^{+/+} (Sigma), mounted on slides using Immu-Mount mounting solution (Thermo Scientific) and imaged immediately with Zeiss LSM 780 confocal microscope.

4.5 | Immunofluorescence staining

Organoids were fixed at day 3 or 6 of culture in cold 100% methanol at RT for 15 to 30 minutes transferred into fresh 100% methanol and stored at -20°C for processing. Before immunostaining, samples were washed twice in 1 \times PBS (Sigma) for 15 to 30 minutes. Then, samples were blocked in 10% goat serum with 1% Triton X-100 in 1 \times PBS for 1 hour at RT. Following blocking, samples were incubated with following antibodies: Aquaporin 1

(#CA0648, rabbit, 1:50, Cell Applications, San Diego, CA, USA), Laminin (#L9393, rabbit, 1:1000, Sigma), Pax2 (#PRB-276P-200, rabbit, 1:200, Covance, Princeton, NJ, USA), Synaptopodin (#BM5086P, mouse IgG₁, 1:4, Acris, Herford, Germany), Wt-1 (#05-753, rabbit, 1:500, Millipore, Burlington, MA, USA), *Lotus Tetragonolobus* lectin (LTL, #FL-1321-2, 1:300, Vector Laboratories, Burlingame, CA, USA), Troma 1 (#AB531826, 1:200, DSHB, Olympia, WA, USA), Six2 (#11562-1AP, 1:200, Proteintech, Manchester, UK) at 4°C ON. On the next day, the samples were washed three times in 1 \times PBS and the secondary antibody was applied: goat anti-rabbit (647, Molecular Probes, Eugene, OR, USA), goat anti-mouse IgG₁ (488 or 546, Molecular Probes), goat anti rat (647, Molecular Probes) for ON incubation at 4°C. The next day, the samples were washed twice 15 minutes with 1 \times PBS, once 5 minutes with 1 \times PBS supplemented with Hoechst 33342 (Thermo Scientific, #H1399) and washed once 15 minutes with 1 \times PBS, then samples were mounted using Immu-Mount mounting solution (Thermo Scientific), and imaged using Zeiss LSM800 confocal microscope, and ZEN software.

4.6 | qPCR

Organoids were collected into Trizol (Life Technologies, Waltham, MA, USA) at day 6 of culture and stored in -20°C until RNA extraction. The total RNA was extracted using standard Trizol/chloroform (Sigma) protocol and cDNA synthesis was performed according to ThermoScientific protocol (cDNA synthesis Kit #K1612). Cycling parameters were as follows: 95°C – 5 min, 95°C – 30 seconds, 62°C – 90 seconds, 40 cycles. The primer sequences are given in Table 2.

4.7 | TEM

Organoids were fixed with mixture of 1% glutaraldehyde and 4% paraformaldehyde in 0.1 M PBS (pH 7.4) for 12 hours at RT and stored at 4°C until processed further. After fixation, the samples were washed once in 0.1 M PBS ON followed by three 20 minutes washes in water. Then, samples were incubated in 1% OsO₄ for 60 minutes, followed by three 10 minutes washes in water and 60 minutes incubation in 1% to 2% uranyl acetate, and three 10 minutes washes in water. Then, the samples were dehydrated through a graded series of acetone solutions and embedded in Epon (Ladd, Wailiston VT, USA). 60 nm thick sections were analyzed on TEM microscope (Tecnaï G2 Spirit, Leica, Wetzlar, Germany).

TABLE 2 List of primers used in the study

Gene	Primer sequence	Source
Slc12a1	F: TCATTGGCCTGAGC GTAGTTG	PrimerBank ID: 1079521a1
	R: TTTGTGCAAATAGC CGACATAGA	
Slc4a4	F: GAAGGTCACCACAC GATCTACA	PrimerBank ID: 9055346a1
	R: TCCACATCAGATTT GTCGGAGT	
Podocin	F: GACCAGAGGAAGGC ATCAAGC	PrimerBank ID: 18485514a1
	R: GCACAACCTTTATG CAGAACCAG	
Oat1	F: CTGATGGCTTCCCA CAACAC	PrimerBank ID: 31982137a1
	R: GTCCTTGCTGTCC AGGGG	
Oat3	F: ATGACCTTCTCCGA GATTCTGG	PrimerBank ID: 31543719a1
	R: GTGGTTGGCTATTC CGAGGAT	
GapDH	F: AGGTCGGTGTGAAC GGATTTG	PrimerBank ID: 6679937a1
	R: TGTAGACCATGTAG TTGAGGTCA	

4.8 | Organic anion transporter assay

Organoids were cultured for 6 days and Oat activity was investigated as described before.⁷ Briefly, organoids were washed with 1× PBS, then incubated twice 5 minutes in PBS^{Ca+Mg+} (Sigma), then control samples were incubated for 1 hour in PBS^{Ca+Mg+} supplemented with both: probenecid (Sigma, #P8761-25G, 200 μM) and 6-CF (Sigma, #C0662-50MG, 10 μM) at 25°C in the dark; while the experimental samples were incubated in PBS^{Ca+Mg+} supplemented with 6-CF only. Following this incubation, samples were washed twice 5 minutes in cold PBS^{Ca+Mg+} and activity of all Oats was blocked by 15 minutes incubation in probenecid solution (800 μM). Following this, samples were mounted and immediately imaged using confocal microscope Zeiss LSM 800 and ZEN software.

4.9 | Data analysis

Analyses were performed either in Excel or in GraphPad Prism on at least three biological experiments. The number of samples used for qPCR in each experiment varied between 6-10 for biggest organoid (30 000-10 000) and

10-20 for smallest organoids (5000 and 2500). The qPCR results were normalized to freshly isolated MM cells.

The total area of the organoids, the induced area (of renal vesicles and more advanced nephrons) and number of developing nephrons, was calculated on day 3 of culture using Fiji (ImageJ2).²⁶ A border was drawn around the specific area and measurements were done automatically by the program. Numerical analysis was performed using Excel.

6-CF fluorescence intensity was measured from three samples in two places each using function “Profile” in ZEN software. One-way analysis of variance was used to find the significant differences between samples, the 30 000 organoid sample was used as a control if not stated otherwise in the text, differences were considered significant at **P* < 0.05, ***P* < 0.001, ****P* < 0.0001 or not significant - # or left unmarked.

ACKNOWLEDGEMENTS

We would like to thank Paula Haipus and Johanna Keholahti-Liias, the BCO Electron Microscopy core facility staff (Ilkka Miinalainen and Sirpa Kellokumpu) and BCO Imaging core facility staff (Veli-Pekka Ronkainen) for their technical assistance. We would also like to thank Dr. Virpi Glumoff for sharing PI staining solution, Dr. Ilya Skovorodkin, Dr. Nsrein Ali, Dr. Zenglai Tan and Dr. Abhishek Sharma for scientific discussions and Dr. Susanna Kosamo for critical reading of the manuscript.

AUTHOR CONTRIBUTIONS

Ganna Reint: Data curation (equal); writing - original draft (equal); writing - review and editing (equal). **Fabienne Geiger:** Data curation (equal); writing - original draft (equal); writing - review and editing (equal). **Florence Naillat:** Data curation (equal); writing - review and editing (equal). **Seppo Vainio:** Conceptualization (equal); funding acquisition (equal); writing - original draft (equal); writing - review and editing (equal).

ORCID

Aleksandra Rak-Raszewska  <https://orcid.org/0000-0002-2399-4410>

REFERENCES

- Saxen L. Inductive interactions in kidney development. *Symp Soc Exp Biol.* 1971;25:207-221.
- Rak-Raszewska A, Hauser PV, Vainio S. Organ in vitro culture: what have we learned about early kidney development? *Stem Cells Int.* 2015;2015:959807-959816.
- Unbekandt M, Davies JA. Dissociation of embryonic kidneys followed by reaggregation allows the formation of renal tissues. *Kidney Int.* 2010;77(5):407-416.

4. Davies JA, Unbekandt M, Ineson J, Lusis M, Little MH. Dissociation of embryonic kidney followed by re-aggregation as a method for chimeric analysis. *Methods Mol Biol.* 2012;886:135-146. https://doi.org/10.1007/978-1-61779-851-1_12
5. Saarela U, Akram SU, Desgrange A, et al. Novel fixed z-direction (FiZD) kidney primordia and an organoid culture system for time-lapse confocal imaging. *Development.* 2017;144(6):1113-1117.
6. Lefevre JG, Chiu HS, Combes AN, et al. Self-organisation after embryonic kidney dissociation is driven via selective adhesion of ureteric epithelial cells. *Development.* 2017;144(6):1087-1096. <https://doi.org/10.1242/dev.140228>
7. Rak-Raszewska A, Wilm B, Edgar D, Kenny S, Woolf AS, Murray P. Development of embryonic stem cells in recombinant kidneys. *Organogenesis.* 2012;8(4):125-136.
8. Huch M, Dorrell C, Boj SF, et al. In vitro expansion of single Lgr5+ liver stem cells induced by wnt-driven regeneration. *Nature.* 2013;494(7436):247-250. <https://doi.org/10.1038/nature11826>
9. Sato T, Vries RG, Snippert HJ, et al. Single Lgr5 stem cells build crypt-villus structures in vitro without a mesenchymal niche. *Nature.* 2009;459(7244):262-265.
10. Boyle S, Misfeldt A, Chandler KJ, et al. Fate mapping using Cited1-CreERT2 mice demonstrates that the cap mesenchyme contains self-renewing progenitor cells and gives rise exclusively to nephronic epithelia. *Dev Biol.* 2008;313(1):234-245.
11. Kobayashi A, Valerius MT, Mugford JW, et al. Six2 defines and regulates a multipotent self-renewing nephron progenitor population throughout mammalian kidney development. *Cell Stem Cell.* 2008;3(2):169-181.
12. Das A, Tanigawa S, Karner CM, et al. Stromal-epithelial crosstalk regulates kidney progenitor cell differentiation. *Nat Cell Biol.* 2013;15(9):1035-1044.
13. Fetting JL, Guay JA, Karolak MJ, et al. FOXD1 promotes nephron progenitor differentiation by repressing decorin in the embryonic kidney. *Development.* 2014;141(1):17-27.
14. Halt KJ, Parssinen HE, Junttila SM, et al. CD146(+) cells are essential for kidney vasculature development. *Kidney Int.* 2016;90(2):311-324.
15. Brown AC, Muthukrishnan SD, Guay JA, et al. Role for compartmentalization in nephron progenitor differentiation. *Proc Natl Acad Sci U S A.* 2013;110(12):4640-4645.
16. Kuure S, Popsueva A, Jakobson M, Sainio K, Sariola H. Glycogen synthase kinase-3 inactivation and stabilization of beta-catenin induce nephron differentiation in isolated mouse and rat kidney mesenchymes. *J Am Soc Nephrol.* 2007;18(4):1130-1139.
17. Drake KA, Chaney CP, Das A, et al. Stromal β -catenin activation impacts nephron progenitor differentiation in the developing kidney and may contribute to wilms tumor. *Development.* 2020;147(21):dev189597. <https://doi.org/10.1242/dev.189597>
18. Junttila S, Saarela U, Halt K, et al. Functional genetic targeting of embryonic kidney progenitor cells ex vivo. *J Am Soc Nephrol.* 2015;26(5):1126-1137.
19. Leclerc K, Costantini F. Mosaic analysis of cell rearrangements during ureteric bud branching in dissociated/reaggregated kidney cultures and in vivo. *Dev Dyn.* 2016;254:483-496.
20. Kojima Y, Tam OH, Tam PP. Timing of developmental events in the early mouse embryo. *Semin Cell Dev Bio.* 2014;34:65-75.
21. Chan AOK, Dong M, Wang L, Chan WY. Somite as a morphological reference for staging and axial levels of developing structures in mouse embryos. *Neuroembryol Aging.* 2004;3:102-110. <https://doi.org/10.1159/000089005>
22. Cebrian C, Asai N, D'Agati V, Costantini F. The number of fetal nephron progenitor cells limits ureteric branching and adult nephron endowment. *Cell Rep.* 2014;7(1):127-137. <https://doi.org/10.1016/j.celrep.2014.02.033>
23. Higgins JW, Chambon A, Bishard K, et al. Bioprinted pluripotent stem cell-derived kidney organoids provide opportunities for high content screening. *bioRxiv.* 2018:505396. <http://biorxiv.org/content/early/2018/12/23/505396.abstract>. <https://doi.org/10.1101/505396>.
24. Borestrom C, Jonebring A, Guo J, et al. A CRISP(e)R view on kidney organoids allows generation of an induced pluripotent stem cell-derived kidney model for drug discovery. *Kidney Int.* 2018;94(6):1099-1110.
25. Rak-Raszewska A. Experimental tubulogenesis induction model in the mouse. *Methods Mol Biol.* 2019;1926:39-51. https://doi.org/10.1007/978-1-4939-9021-4_4
26. Sun Z, Wang Y, Ji S, Wang K, Zhao Y. Computer-aided analysis with image J for quantitatively assessing psoriatic lesion area. *Skin Res Technol.* 2015;21(4):437-443. <https://doi.org/10.1111/srt.12211>

How to cite this article: Rak-Raszewska A, Reint G, Geiger F, Naillat F, Vainio SJ. Deciphering the minimal quantity of mouse primary cells to undergo nephrogenesis ex vivo. *Developmental Dynamics.* 2022;251(3):536-550. doi: 10.1002/dvdy.418